JPE 15-3-3

http://dx.doi.org/10.6113/JPE.2015.15.3.602
ISSN(Print): 1598-2092 / ISSN(Online): 2093-4718

# A ZCT Double-Ended Flyback Converter with Low EMI

Mohammad Rouhollah Yazdani[†], Saeid Rahmani[*], and Mehdi Mohammadi[**]

[†]Department of Electrical Engineering, Isfahan (Khorasgan) Branch, Islamic Azad University, Isfahan, Iran
[*]Department of Electrical and Computer Engineering, Najaf Abad Branch, Islamic Azad University, Isfahan, Iran
[**]Department of Electrical and Computer Engineering, University of British Columbia, Vancouver, Canada

## Abstract

In this paper, a zero current transition (ZCT) double-ended flyback converter is proposed. All of the switching elements act under soft switching conditions and the voltage stress of the main switches is limited to the input voltage due to the innate behavior of the double-ended flyback converter. Providing soft switching conditions and clamping the voltage stress improves the efficiency and electromagnetic compatibility (EMC). The Proposed converter is analyzed in detail and its operating modes are discussed in detail. Experimental results are presented to verify the theoretical predictions. Moreover, the conducted electromagnetic emissions of the proposed ZCT double-ended flyback converter are measured to show another merit of the proposed converter in addition to providing soft switching conditions. The measured electromagnetic interference (EMI) of the proposed converter demonstrates that its EMI is lower than the conventional double-ended flyback converter. Furthermore, two simple and cost effective EMI reduction methods are applied to satisfy the EMC standard.

**Key words:** Double-ended flyback converter, EMC, EMI, Soft switching, ZCT

## I. INTRODUCTION

Today, power switching converters are widely used in many applications such as fuel cells [1], LED drivers [2], power factor correction [3] and photovoltaic systems [4]. Among the various switching converters, the flyback topology is widely used in electronic systems due to its benefits such as isolation and a simple structure. The best way to decrease the weight and size of a converter is to increase the switching frequency. Due to the non-ideal behavior of the semiconductor elements used in power converters, increasing the switching frequency may lead to increases in both switching losses and electromagnetic interference (EMI). It may also drive the converter switch out from the safe operating area (SOA). Over the years, many methods have been introduced to diminish these problems. Generally, soft switching techniques including both passive and active methods are commonly used to counteract the repercussions of increasing the switching frequency in PWM converters. Because passive snubber circuits use no additional active components to provide soft switching conditions, they usually do not increase the complexity of the control and gate drive circuits. In [5], a lossless passive snubber cell is introduced which can be engaged on double-ended flyback converters. However, the number of components in each cell is high. In addition, because two snubber cells should be applied for each converter switch, the converter power conversion density is affected. In [6], a lossless passive snubber is suggested for double-ended flyback converters. When the converter switch is on, the current through the snubber inductors freewheels through the converter switches and the two snubber diodes. This causes the conductive losses to increase. In addition, the number of the snubber components is relatively high. In [7], a half bridge interleaved flyback converter is introduced which uses a simple lossless passive snubber cell. Although, the snubber circuit is simple, two snubber cells should be used for the two converter switches. Moreover, two distinct cores must be engaged in this converter.

Manuscript received Aug. 3, 2014; accepted Jan. 9, 2015
Recommended for publication by Associate Editor Bor-Ren Lin.
[†]Corresponding Author: mro.yazdani@gmail.com
Tel: +98-31-35354001, Fax: +98-31-35354060, Isfahan (Khorasgan) Branch, Islamic Azad University
[*]Department of Electrical and Computer Engineering, Najafabad Branch, Islamic Azad University, Iran.
[**]Department of Electrical and Computer Engineering, University of British Columbia (UBC), Canada.

Passive snubbers are usually able to achieve zero voltage and zero current switching conditions at the turning off and on moments, respectively. However, some active methods provide zero voltage and zero current transition (ZVT and ZCT) conditions at the turning on and off instants, respectively [8], [9]. In addition to these methods, forcing the converter to work in critical conduction mode (CRM) can lead to soft switching conditions. Although, working under this condition decreases the switching losses, it increases the conduction losses due to an increased rms current. In addition, the CRM results in a more complicated control circuit than regular converters. Moreover, the switching frequency cannot be constant which results in a non-optimum filter design.

Among the isolated converters, the flyback converter has a low cost and simple structure [10]. Despites, the advantages of the single-switch flyback topology, it has some disadvantages which make it difficult to be used especially in medium power applications. The switch voltage stress and the voltage spikes caused by the transformer leakage inductor ($L_{lk}$) are two major problems of the conventional single-switch flyback converter. In addition, switching losses and EMI are concerns that should be considered. The double-ended flyback converter clamps switch voltage stress to the input voltage. Furthermore, recycling the $L_{lk}$ energy to the input voltage significantly reduces the voltage spikes across the converter switches. In addition to the switch stress and switching losses reduced by soft switching techniques, the EMI is an important parameter that should be taken into consideration in soft switching converters. Unwanted resonances and other parasitic elements due to an increased component quantity may lead to insufficient EMI reduction in some soft switching converters. In [11], a ZCT single-switch flyback converter with a simple auxiliary cell at the secondary side of the transformer is introduced. The auxiliary switch voltage suffers from voltage spikes at the turn-off instant which affects the electromagnetic emissions [12]. In [13], a double-ended ZCT flyback converter with an auxiliary cell at the secondary side of the transformer is proposed. Although, it is desirable to apply soft switching cells with a minimum need for isolated gate drive circuits, three isolated gate drivers must be used in [13]. In addition, there are considerable high frequency oscillations in the waveforms of the main and auxiliary switches which may result in more common-mode (CM) and differential-mode (DM) EMI. CM EMI is generated with high *di/dt* and *dv/dt* across the parasitic elements between the circuit and the chassis (earth). An important CM impedance is the capacitance between the switch drain and the earth ($C_{DE}$) including the heat-sink capacitance [14]. In the double-ended flyback converter, the drain of the upper switch is connected to the DC input voltage and consequently its $C_{DE}$ is not important from the EMI viewpoint. Due to providing soft switching conditions via the suggested snubber cell, the impact of the lower switch's $C_{DE}$ on the EMI is limited.

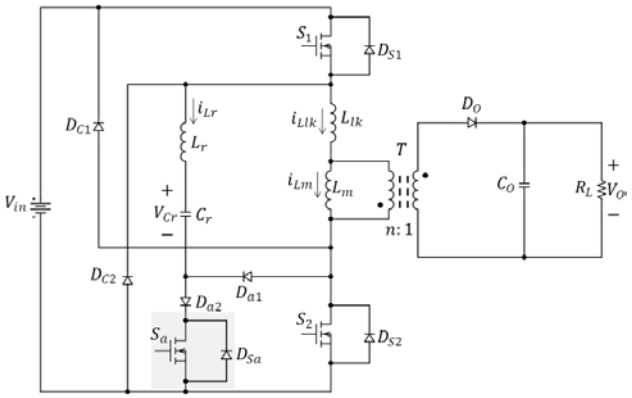

Fig. 1. The proposed ZCT double-ended flyback converter

In this paper, a double-ended flyback converter with an active auxiliary cell is introduced which causes the converter switches to be turned off under the ZCT condition. Due to the transformer leakage inductor, the converter switches are turned on under the ZCS condition. In addition, the voltage stress of the main switches is clamped to the input voltage. Clamping the voltage stress leads to lower voltage across the switches. Generally, MOSFETs with a lower voltage have a lower ON resistance. Using these MOSFETs will reduce the conductive losses. In the proposed converter, the EMC can be also improved by providing the ZC condition at the turn off instant. In the proposed converter because the switching frequency is relatively high, the size is reduced. In addition, the switching losses are decreased due to providing soft switching conditions. The auxiliary snubber cell is responsible in obtaining this condition. Moreover, In the proposed topology only one floating gate drive circuit is needed. As a result, in this the case boot strap technique can be used to drive the upper switch to prevent the use of a pulse transformer or an optocoupler.

This paper is arranged into five sections. In section II, the proposed ZCT double-ended flyback converter is discussed in detail. Section III provides an appropriate design procedure for the active auxiliary snubber cell. In order to justify the theoretical discussions about the proposed converter, section IV presents some experimental results. In section V, conducted EMI measurements of the converter are presented. Finally, in section VI the remarkable points of the aforementioned discussions are presented.

## II. THE PROPOSED CONVERTER

In Fig. 1, the proposed ZCT double-ended flyback converter is shown. The auxiliary circuit is made up of $L_r$, $C_r$, $S_a$, $D_{a1}$ and $D_{a2}$. The proposed converter in each switching period has 10 operating intervals which are discussed in detail below. Fig. 2 shows the equivalent circuits of each interval, and Fig. 3 shows the important theoretical waveforms of the proposed converter. Before explaining the operating modes, it is assumed that the

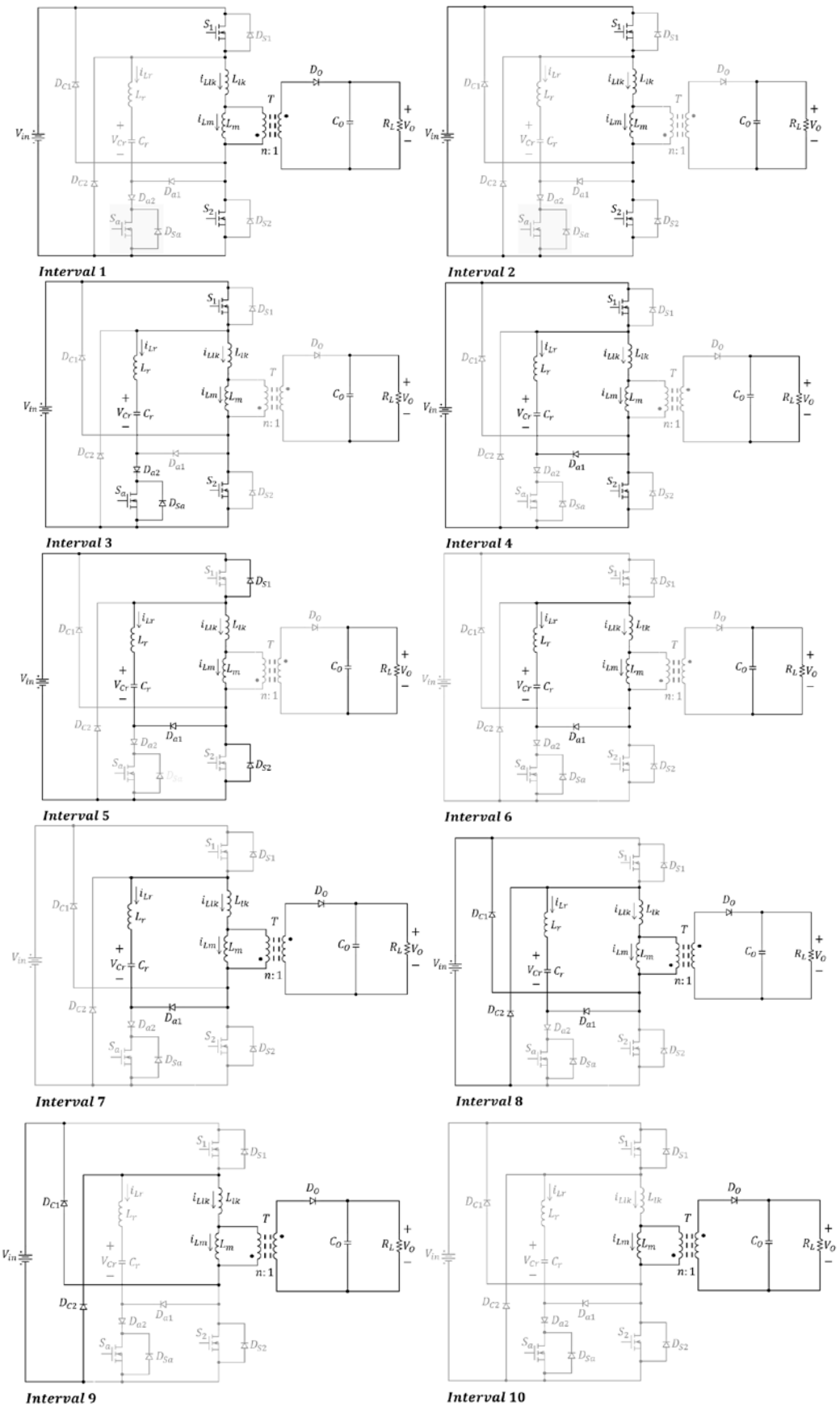


Fig. 2. The equivalent circuits of each operating mode.

converter switches $S_1$ and $S_2$ along with the auxiliary switch $S_a$ are all off, all of the diodes except $D_O$ are off, and $V_{Cr}$ is $V_{Cr}(t_0)$. In this case the transformer magnetizing inductor $L_m$ is transferring its stored energy to the output voltage.

***Interval 1 [$t_0$–$t_1$]***: At $t_0$ the converter switches $S_1$ and $S_2$ are simultaneously turned on under the ZC condition, due to the transformer leakage inductor $L_{lk}$. In this interval, because the current through $L_{lk}$ is lower than $I_{Lm}$, $D_O$ remains on and so the voltage of $V_{in}+nV_O$ is placed across $L_{lk}$ which causes its current to increase linearly. The important equations of this interval are as follows:

$$i_{Llk}(t) = \frac{V_{in} + nV_O}{L_{lk}}(t - t_0) \tag{1}$$

$$i_{Lm}(t) = i_{Lm}(t_0) - \frac{nV_O}{L_m}(t - t_0) \tag{2}$$

***Interval 2 [$t_1$–$t_2$]***: At $t_1$ the current of $L_{lk}$ is equal to the current through $L_m$. At the beginning of this mode, $D_O$ turns off under the ZC condition. The operation of the proposed converter in this interval is the same as that in the conventional flyback converter where $L_m$ is being charged via the input DC voltage. The important equation of this interval is as follows:

$$i_{Llk}(t) = i_{Lm}(t) = i_{Lm}(t_1) + \frac{V_{in}}{L_{lk} + L_m}(t - t_1) \tag{3}$$

***Interval 3 [$t_2$–$t_3$]***: To turn the main converter switches off under the ZC condition, the auxiliary cell should reduce their currents to zero. Therefore, at $t_2$, $S_a$ is turned on under the ZC condition. Turning $S_a$ on starts a resonance between $L_r$ and $C_r$. The important equations of this interval are as follows:

$$i_{Lr}(t) = \frac{V_{in} + V_{Cr}(t_0)}{L_r \omega_0} Sin(\omega_0 (t - t_2)) \tag{4}$$

$$V_{Cr}(t) = V_{Cr}(t_0) - [V_{in} + V_{Cr}(t_0)][Cos(\omega_0 (t - t_2)) - 1] \tag{5}$$

where:

$$\omega_0 = \frac{1}{\sqrt{L_r C_r}} \tag{6}$$

***Interval 4 [$t_3$–$t_4$]***: At $t_3$, after half of the resonance is started in interval 3, the current through $L_r$ wants to flow in the opposite direction. Due to $D_{a2}$, which is installed in series with $S_a$, the current cannot flow through $S_a$. Therefore, $S_a$ and $D_{a2}$ turn off under the ZC condition. Therefore, $D_{a1}$ turns on under the ZC condition. In this mode the current of $L_r$ and the voltage of $C_r$ can be calculated via equations (4) and (5), respectively.

***Interval 5 [$t_4$–$t_5$]***: At $t_4$, $I_{Lr}$ reaches $I_{Lm}$ and causes the current through $S_1$ and $S_2$ to become zero. Then, the current thorough $L_r$ increases more than $I_{Lm}$. When $I_{Lr}$ is higher than $I_{Lm}$, the converter switches $S_1$ and $S_2$ can be turned off under the ZCS condition. Turning $S_1$ and $S_2$ off causes the body diodes $D_{S1}$ and $D_{S2}$ to turn on under the ZV condition. Thus, the resonance between $C_r$ and $L_r$ continues through the provided pass via $D_{S1}$ and $D_{S2}$.

***Interval 6 [$t_5$–$t_6$]***: At the beginning of this interval, the current through $L_r$ reaches $I_{Lm}$ again. As a result, $D_{S1}$ and $D_{S2}$ turn off under the ZC condition. In this mode, a new resonance occurs between $C_r$, $L_r$, $L_{lk}$ and $L_m$. Because $L_m$ is very large with respect to $L_{lk}$ and $L_r$; during this interval, it can be assumed that $C_r$ is charged with a constant current. The important equation of this mode is as follows:

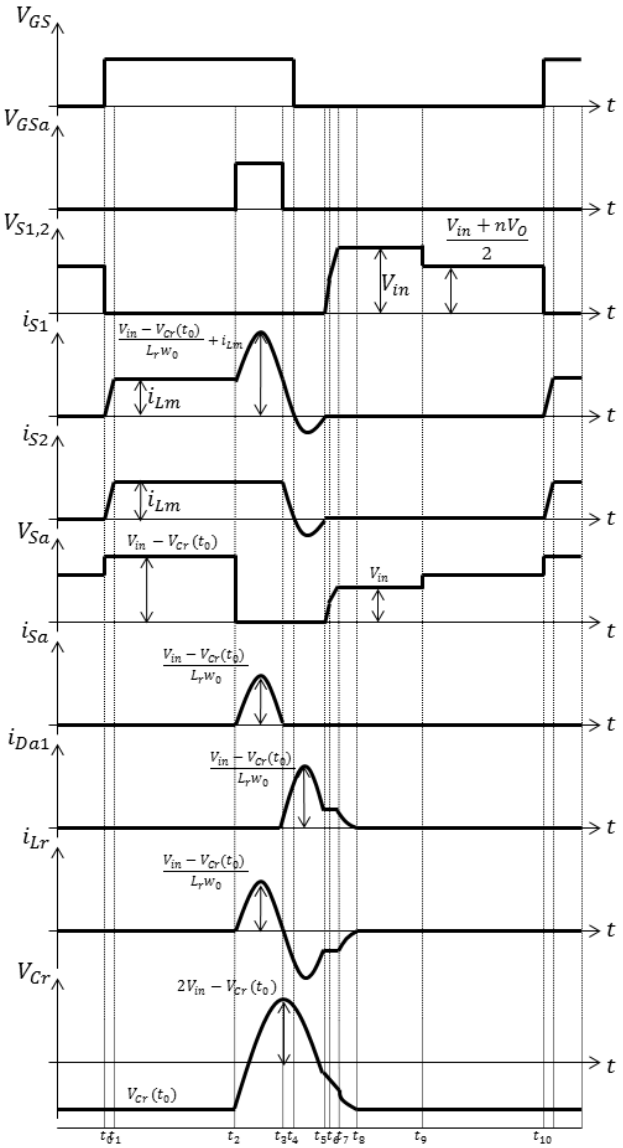


Fig. 3. Theoretical waveforms of the proposed converter.

$$V_{Cr}(t) = V_{Cr}(t_5) - \frac{i_{Lm}(t_5)}{C_r}(t - t_5) \tag{7}$$

*Interval 7 [$t_6$-$t_7$]*: At $t_6$, the voltage of $C_r$ reaches $-[1 + (L_{lk} + L_r)/L_m]nV_O$. As a result, $D_O$ turns on. In this interval a new resonance starts between $L_{lk}$, $L_r$ and $C_r$.

$$i_{Lr}(t) = i_{Llk}(t) = \frac{nV_O}{\omega_1 L_m} Sin(\omega_1 (t - t_6)) - i_{Lr}(t_6) Cos(\omega_1 (t - t_6)) \tag{8}$$

$$V_{Cr}(t) = -nV_O + \frac{i_{Lr}(t_6)}{C_r \omega_1} Sin(\omega_1 (t - t_6)) - \frac{L_{lk} + L_r}{L_m} nV_O Cos(\omega_1 (t - t_6)) \tag{9}$$

where:

$$\omega_1 = \frac{1}{\sqrt{(L_{lk} + L_r) C_r}} \tag{10}$$

***Interval 8 [$t_7$-$t_8$]***: At $t_7$, the voltage of $C_r$ reaches $-(1 + L_r / L_{lk})V_{in} + (L_r / L_{lk})nV_O$. On the other hand, the voltages

of the converter switches $S_1$ and $S_2$ become $V_{in}$. Thus, $D_{C1}$ and $D_{C2}$ turn on under the ZV condition. In this interval, a voltage of $V_{in}$-$nV_O$ drops across $L_{lk}$ inversely and its current decreases linearly. In addition, in this mode a resonance occurs between $L_r$ and $C_r$. Under this resonance the current through $L_r$ is reduced. The important equations of this mode are as follows:

$$i_{Llk}(t) = i_{Llk}(t_7) - \frac{V_{in} - nV_O}{L_{lk}}(t - t_7) \quad (11)$$

$$i_{Lr}(t) = -i_{Lr}(t_7)Cos(\omega_0(t - t_7)) + \frac{V_{in} + V_{Cr}(t_7)}{L_r\omega_0}Sin(\omega_0(t - t_7)) \quad (12)$$

$$V_{Cr}(t) = \frac{i_{Lr}(t_7)}{C_r\omega_0}Sin(\omega_0(t - t_7)) - [V_{in} - V_{Cr}(t_7)]Cos(\omega_0(t - t_7) + V_{in} \quad (13)$$

***Interval 9 [$t_8$-$t_9$]***: At $t_8$, $I_{Lr}$ reaches zero and $D_{a1}$ turns off under the ZC condition. In this mode, $L_{lk}$ still has energy. As a result, $D_{C1}$ and $D_{C2}$ remain on. During this interval, the current through $L_{lk}$ can be calculated with Equ. (11).

***Interval 10 [$t_9$-$t_{10}$]***: At $t_9$, $I_{Llk}$ becomes zero. As a result, $D_{C1}$ and $D_{C2}$ turn off under the ZC condition. The operation of the proposed converter in this mode is the same as that in the conventional double-ended flyback converter.

## III. Design Guidelines

There are two parts to the design of the proposed double-ended flyback converter. The first part is the design of the power section and the second part is the calculation of the values of the snubber components. The first part can be computed in the same way as any conventional flyback converter [15]. In this section a simple approach to choose proper values for the auxiliary cell is introduced. In order to achieve the ZC condition at the turning off instant for the main converter switches, two criteria should be considered. The first criterion is that the resonant period starting in interval 3 must be smaller than the minimum switch on time. Therefore, $\omega_0$ should be chosen with equation (14).

$$\omega_0 > \frac{2\pi f_{sw}}{\underline{D}} \quad (14)$$

where $f_{sw}$ and $\underline{D}$ are the switching frequency and the minimum duty cycle, respectively.

The second criterion is that the maximum resonant current starting in interval 3 must be larger than $I_{Lm}$ at the maximum output power. As a result, equation (15) can be used to calculate $L_r$.

$$L_r < \frac{C_r(V_{in} + V_C(t_0))^2}{\overline{I_{Lm}}^2} \quad (15)$$

where $\overline{I_{Lm}}$ is the maximum current of $L_m$ at the maximum output power. In addition, as discussed in section II, at the end of Interval *7*, the voltage of $C_r$ is nearly equal to $-V_{in}$. Therefore, this quantity is a good estimation of $V_C(t_0)$. By using Equations (14) and (15), $C_r$ and $L_r$, can be calculated. In addition, to compute $\overline{I_{Lm}}$ at the maximum output power, the equation below can be used.

$$\overline{I_{Lm}} = \eta\left(\frac{\overline{P_O}}{\overline{V_{in}}\underline{D}} + \frac{\overline{V_{in}}\underline{D}}{2L_m f_{sw}}\right) \quad (16)$$

where $\overline{P_O}$, $\eta$ and $f_{sw}$ are the nominal power of the converter, the converter efficiency, and the switching frequency. In the worst case, the efficiency while considering an over design can be selected as 0.8.

Another parameter for designing the proposed converter is the selection of appropriate semiconductor elements. The voltage stresses of the main components are shown in Table I. To simplify the calculation of $V_{Cr}(t_0)$, it is assumed that the resonance between $C_r$ and $L_r$ is complete. Meanwhile, the converter works between Modes 3 to 8. Therefore, $V_{Cr}(t_0)$ can be obtained by Equation (5). Based on this assumption, its value is around $-V_{in}$.

TABLE I
Voltage Stresses of Main Semiconductor Components

| Component | Voltage Stress |
|---|---|
| $S_1$ and $S_2$ | $V_{in}$ |
| $S_a$ | $V_{in}$ -$V_{Cr}(t_0)$ |
| $D_O$ | $V_{in}/n+V_O$ |
| $D_{C1}$ and $D_{C2}$ | $V_{in}$ |
| $D_{a1}$ | $V_{in}$ -$V_{Cr}(t_0)$ |
| $D_{a2}$ | $V_{in}$ -$V_{Cr}(t_0)$ |

## IV. Experimental Results

To assess the theoretical analysis of the proposed converter, a *60W* prototype of a ZCT double-ended flyback converter is implemented with a *100 kHz* switching frequency. The input and output voltages are *75V* and *24V*, respectively. The $L_m$ and $L_{lk}$ values are *590μH* and *9uH* and the turns ratio of the transformer is *2.32*. $L_r$ and $C_r$ are chosen as *16μH* and *4.7nF* based on the design procedure introduced in the previous section. *IRF540*s are utilized for the switches and a *BYV32-200* and *UF4001*s are used as the output diode $D_O$ and snubber diodes, respectively.

Fig. 4 shows the experimental waveforms of the voltage and current of $S_2$ and the voltage of the auxiliary switch $S_a$. In Fig. 4(a) it is evident that $S_2$ is turned on and off under the ZC condition. Fig. 4(b) shows the voltage and current of the auxiliary switch $S_a$ to demonstrate that the switch acts under the soft switching conditions during transition times. The switch voltage stress of $S_1$ and $S_2$ is clamped to the input voltage which prevents fluctuations after turning the switches off. This reduces the electromagnetic emissions of the converter to [12]. To demonstrate that the soft switching condition for the proposed converter has the ability to improve the converter efficiency, the converter efficiency curve is depicted in Fig. 5. To compare the proposed converter in terms

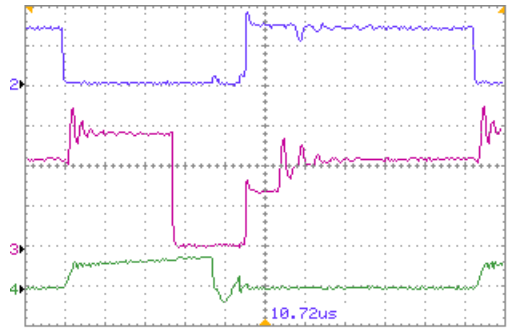


(a)

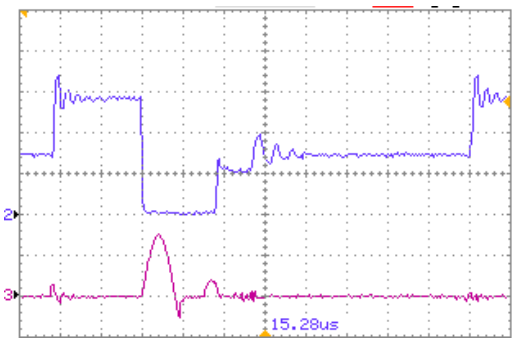


(b)

Fig. 4. (a) Top: $S_2$ voltage, Middle: $S_a$ voltage, Bottom: $S_2$ current. (ver. scale: 2.5 A/div or 50 V/div; time scale: 1 µs/div). (b) Top: $S_a$ voltage, Bottom: $S_a$ current. (ver. scale: 2 A/div or 50 V/div; time scale: 1 µs/div).

of efficiency, the efficiency curves of the soft switching converter introduced in [6] and the soft switching double-ended flyback converter with are RCD snubber, are also illustrated in Fig. 5. It should be mentioned that the specifications of the mentioned converters are same as the specifications of the proposed converter. It can be seen that the proposed soft switching cell improves the converter efficiency by more than *8%* at the nominal output power with respect to the regular converters. It can also be seen that it has better efficiency in low powers than the converter introduced in [6]. In addition, when compared to [13], the proposed ZCT converter has better efficiency. It should be mentioned that the efficiency improvement of the proposed converter can be increased by using a unidirectional switch instead of $S_a$ and $D_{a2}$ to eliminate $D_{a2}$ losses.

## V. CONDUCTED EMI MEASUREMENT

To examine the conducted EMI reduction, the conducted electromagnetic emissions of the proposed converter are measured and compared with those of a conventional double-ended flyback converter. In addition, to show the benefits of the proposed converter from the EMC viewpoint, the soft switching double-ended converter introduced in [13] was made and its electromagnetic emissions were measured. To measure the EMI, a line impedance stabilization network (*LISN*) based on the *CISPR 22* standard is placed between the

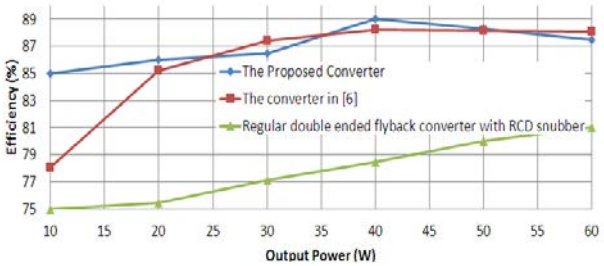


Fig. 5. The efficiency curves.

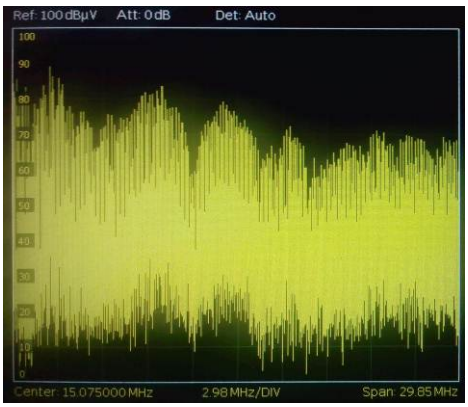


(a)

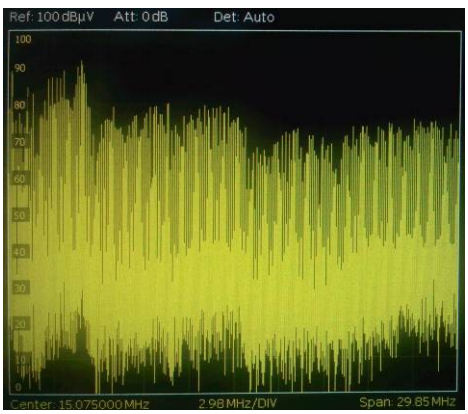


(b)

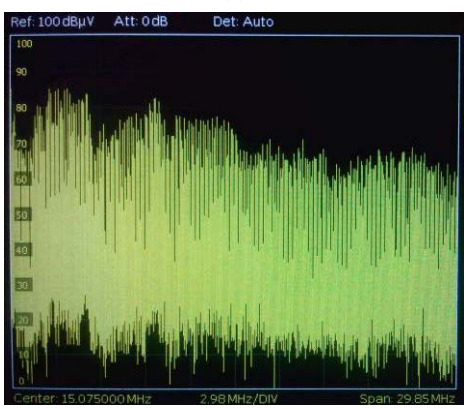


(c)

Fig. 6. Conducted EMI Measurement of double-ended flyback converters. (a) Hard switching (b) ZCT [13] (c) Proposed ZCT (Vertical axis: 0-100dBµV, Horizontal. axis: 150k-30MHz).

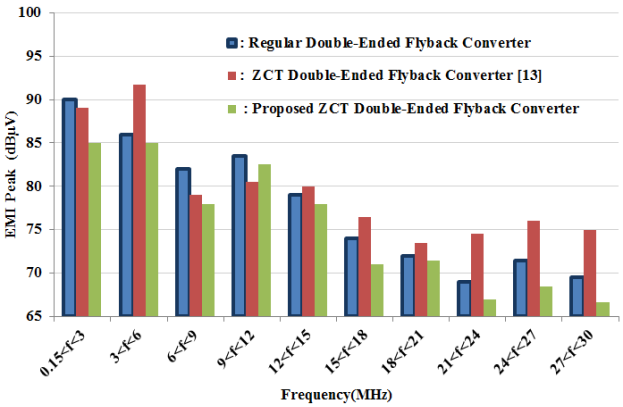


Fig 7. Comparison of EMI measurement for various frequency ranges.

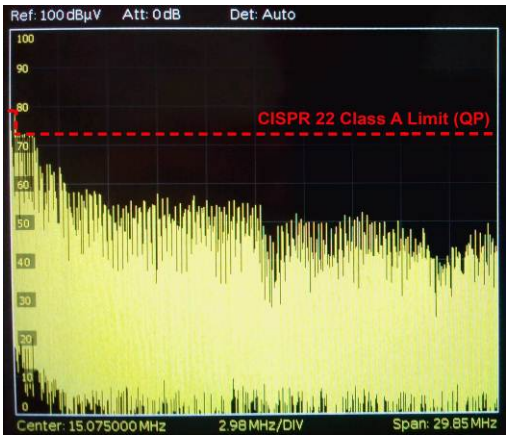


Fig. 8. EMI reduction after applying Faraday shield and CM choke.

input of the converter and the input source lines [16]. The conducted EMI spectrum of the proposed ZCT converter, its hard switching counterpart and the ZCT converter in [13] are measured via a *HAMEG* spectrum analyzer (peak detection mode) as shown in Fig. 6.

Fig. 6 indicates that the main EMI peak of the proposed converter is about *5 dBμV* lower than the main EMI peak of its hard switching counterpart in the total frequency band. In addition, the main EMI peak of the proposed converter is around *7 dBμV* lower than the main EMI peak of the ZCT converter introduced in [13]. To compare the conducted EMI in various frequency ranges, the EMI of the proposed converter along with the hard switching counterpart and the suggested converter in [13] are shown in Fig. 7. Comparing these three converters, the conducted EMI levels of the proposed converter are reduced.

To study the effect of output power variations on the conducted EMI levels, the conducted EMI spectrums for various output powers are measured. Although there are small variations in the EMI levels in some frequencies, the main EMI peaks have no considerable changes for various output powers. Since the proposed converter has a lower main EMI peak, it has the potential to meet the EMC standard via simple and cost-effective EMI reduction methods. One of the EMI reduction methods which can be used for this is a Faraday shield. In this technique, the value of the parasitic capacitor between two the sides of the converter transformer is decreased with a piece of aluminum foil placed between the primary and secondary transformer windings [12]. Another simple method to reduce EMI is to use a common-mode choke at the input of the converter. A common-mode (CM) choke provides a high impedance pass at the input of the converter which improves the converter EMI. The EMI spectrum of the proposed converter with a Faraday shield and a CM choke (with two coupled 300 μH inductance) is depicted in Fig. 8.

Although the EMI peak of the proposed converter is near the limit of *CISPR22* Class A QP (Quasi peak) at low frequencies, this standard is satisfied by the proposed ZCT double-ended flyback converter with two simple EMI reduction techniques. It should be mentioned that the CISPR 22 standard is not satisfied by the regular double-ended converter with these two EMI reduction methods due to its high EMI levels.

## VI. Conclusion

In this paper, a ZCT double-ended flyback converter is introduced in which all of the semiconductor elements act under soft switching conditions. The performance of the proposed converter is investigated in detail and experimental results are offered to verify the theoretical analysis. The engaged active auxiliary cell improves both the converter efficiency and the EMI. Since the achieved soft switching conditions significantly reduce the converter EMI, the proposed converter can satisfy the *CISPR22* standard by simple and cost-effective EMI reduction methods. A Faraday shield and a CM choke (simple EMI reduction methods) are applied to the converter to satisfy the *CISPR22* standard. The results of the EMI measurements verify *CISPR22* satisfaction after applying these two simple methods.

## References

[1] M. Ordonez and J. E. Quaicoe, "Soft-switching techniques for efficiency gains in full-bridge fuel cell power conversion," *IEEE Trans. Power Electron.*, Vol. 2, No. 2, pp. 482-492, Feb. 2011.

[2] J. I. Kang, S. K. Han, and J. Han, "Analysis and design of high-efficiency boundary conduction mode tapped-inductor boost LED driver for mobile products," *Journal of Power Electronics*, Vol. 14, No. 4, pp. 632-640, Jul. 2014.

[3] A. M. Obais and J. Pasupuleti, "Automatic power factor correction using a harmonic-suppressed TCR equipped with a new adaptive current controller," *Journal of Power Electronics*, Vol. 14, No. 4, pp. 742-753, Jul. 2014.

[4] J. P. Lee, B. D. Min, and D. W. Yoo, "Implementation of a high efficiency grid-tied multi-level photovoltaic power conditioning system using phase shifted H-bridge

modules," *Journal of Power Electronics*, Vol. 13, No. 2, pp. 296-303, Mar. 2013.
[5] R. T. H. Li and H. S.-h. Chung, "A passive lossless snubber cell with minimum stress and wide soft-switching range," *IEEE Trans. Power Electron*., Vol. 25, No. 7, pp. 1725-1738, Jul. 2010.
[6] M. Mohammadi, E. Adib, and H. Farzanehfard, "Lossless passive snubber for double-ended flyback converter with passive clamp circuit," *IET Power Electron.*, Vol. 7, No. 2, pp. 245-250, Feb. 2014.
[7] M. Mohammadi and E. Adib, "Lossless passive snubber for half bridge interleaved flyback converter," *IET Power Electron.*, Vol. 7, No. 6, pp. 1475-1481, Jun. 2014.
[8] B. Akın, "An improved ZVT-ZCT PWM DC-DC boost converter with increased efficiency," *IEEE Trans. Power Electron.*, Vol. 29, No. 4, pp. 1919-1926, Apr. 2014.
[9] N. Altintas, A. Faruk Bakan, and I. Aksoy, "A novel ZVT-ZCT-PWM boost converter," *IEEE Trans. Power Electron.*, Vol. 29, No. 1, pp. 256-265, Jan. 2014.
[10] D.-H. Kim and J.-H. Park, "High efficiency step-down flyback converter using coaxial cable coupled-inductor," *Journal of Power Electronics*, Vol. 13, No. 2, pp. 214-222, Mar. 2013.
[11] E. Adib and H. Farzanehfard, "Family of isolated zero current transition PWM converters," *Journal of Power Electronics*, Vol. 9, No. 2, pp. 156-163, Mar. 2009.
[12] M. R. Yazdani, H. Farzanehfard, and J. Faiz, "Classification and comparison of EMI mitigation techniques in switching power converters – A review," *Journal of Power Electronics*, Vol. 11, No. 5, pp. 767-777, Sep. 2011.
[13] D. Murthy-Bellur and M. K. Kazimierczuk, "Zero-current-transition two-switch flyback pulse-width modulated DC-DC converter," *IET Power Electron*., Vol. 4, No. 3, pp. 288-295, Mar. 2011.
[14] R. Vimala, K. Baskaran, and K. R. Aravind Britto "Modeling and filter design through analysis of conducted EMI in switching power converters," *Journal of Power* Electronics, Vol. 12, No. 4, pp. 632-642, Jul. 2012.
[15] A. I. Pressman, *Switching Power Supply Design*, 2nd ed., McGraw- Hill, 1998.
[16] *Information technology equipment – Radio disturbance characteristics – Limits and methods of measurement – Publication 22, IEC International Special Committee on Radio Interference (CISPR)*, 1997.

**Mohammad Rouhollah Yazdani** was born in Isfahan, Iran, in 1978. He received his B.S. degree from the Isfahan University of Technology, Isfahan, Iran, in 2001, his M.S. degree from the Islamic Azad University of Najafabad, Najafabad, Iran, in 2004, and his Ph.D. degree from the Islamic Azad University, Sciences and Research Branch, Tehran, Iran, in 2011, all in Electrical Engineering. Since 2011, he has been a Faculty Member in the Department of Electrical and Computer Engineering, Isfahan (Khorasgan) Branch, Islamic Azad University, Isfahan, Iran. His current research interests include soft-switching converters, EMI modeling and reduction techniques, signal integrity and EMC issues.

**Saeid Rahmani** was born in Fraydan, Isfahan, Iran, in 1987. He received his B.S. and M.S. degrees from the Najafabad Branch, Islamic Azad University, Isfahan, Iran, in 2011 and 2013, respectively. His current research interests include soft-switching converters and EMI.

**Mehdi Mohammadi** was born in Isfahan, Iran, in 1989. He received his A.S. degree from Shahid Mohajer Technical Institution of Isfahan, Isfahan, Iran, in 2008, his B.S. degree from the Bonyan Institute of Higher Education, Shahinshahr, Iran, in 2010, and his M.S. degree from the Isfahan University of Technology, Isfahan, Iran, in 2014, all in Electrical Engineering. He is presently working toward his Ph.D. degree in Electrical Engineering at the University of British Columbia, Vancouver, BC, Canada, where he is involved in finding advanced control methods for power converters and new switching topologies. His current research interests include advanced control schemes for power converters, high-frequency soft-switching converters and their applications, and EMI.